Domain Decomposition of Stocha SAND2018-7957C *Developments*

Ajit Desai [1], Mohammad Khalil [2], Chris Pettit [3], Dominique Poirel [4]
and Abhijit Sarkar [1]

[1]Department of Civil and Environmental Engineering
Carleton University, Canada
[2]Quantitative Modeling & Analysis
Sandia National Laboratories, Livermore, California 94551, USA
[3]Aerospace Engineering Department
United States Naval Academy, Annapolis, Maryland, USA
[4]Department of Mechanical and Aerospace Engineering
Royal Military College of Canada

Sandia National Laboratories is a multimission laboratory managed and operated by National Technology and Engineering Solutions of Sandia, LLC., a wholly owned subsidiary of Honeywell International, Inc., for the U.S. Department of Energy's National Nuclear Security Administration under contract DE-NA-0003525.

July 19, 2017

Introduction

- Motivation
  - Data assimilation for high resolution numerical models.
- Objective
  - Develop scalable parallel algorithms for sequential data assimilation.

    Scalability: Solve n-times larger problem using n-times more processors/cores without substantially increasing the execution time.
- Methodology
  - Exploit scalable intrusive polynomial chaos expansion-based non-overlapping domain decomposition for distributed implementation of data assimilation algorithms.

Bayesian Estimation using Nonlinear Filtering

- Model Equation

$$\mathbf{u}_{k+1} = \psi_k(\mathbf{u}_k, \mathbf{f}_k, \mathbf{q}_k) \quad -- \quad \text{Forecast Step}$$

- Measurement Equation

$$\mathbf{d}_k = \mathbf{h}_k(\mathbf{u}_k, \epsilon_k) \qquad -- \quad \text{Assimilation Step}$$

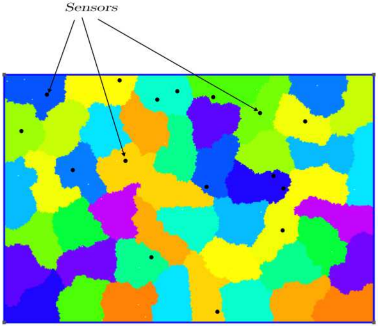

UQ Framework

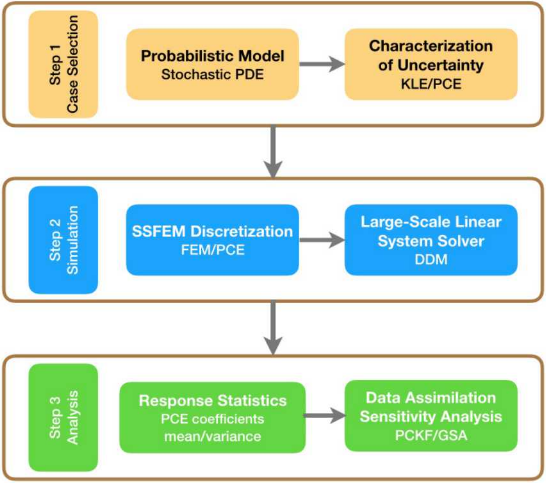

UQ Framework

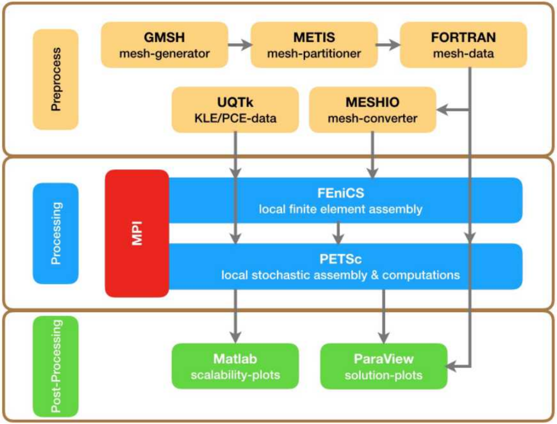

(*Forecast Step*)

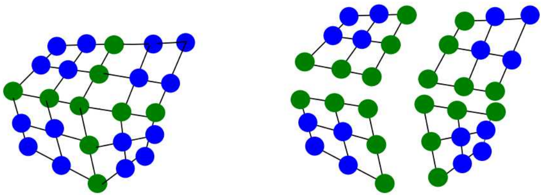

- Spatial decomposition

$$\begin{bmatrix} \mathbf{A}^s_{II}(\theta) & \mathbf{A}^s_{I\Gamma}(\theta) \\ \mathbf{A}^s_{\Gamma I}(\theta) & \mathbf{A}^s_{\Gamma\Gamma}(\theta) \end{bmatrix} \begin{Bmatrix} \mathbf{u}^s_I(\theta) \\ \mathbf{u}^s_\Gamma(\theta) \end{Bmatrix} = \begin{Bmatrix} \mathbf{f}^s_I \\ \mathbf{f}^s_\Gamma \end{Bmatrix} .$$

- Polynomial Chaos expansion

$$\sum_{i=0}^{L} \Psi_i \begin{bmatrix} \mathbf{A}^s_{II,i} & \mathbf{A}^s_{I\Gamma,i} \\ \mathbf{A}^s_{\Gamma I,i} & \mathbf{A}^s_{\Gamma\Gamma,i} \end{bmatrix} \begin{Bmatrix} \mathbf{u}^s_I(\theta) \\ \mathbf{u}^s_\Gamma(\theta) \end{Bmatrix} = \begin{Bmatrix} \mathbf{f}^s_I \\ \mathbf{f}^s_\Gamma \end{Bmatrix} .$$

- Galerkin projection

$$\begin{bmatrix} \mathcal{A}_{II}^{1} & \dots & 0 & \mathcal{A}_{I\Gamma}^{1}\mathcal{R}_1 \\ \vdots & \ddots & \vdots & \vdots \\ 0 & \dots & \mathcal{A}_{II}^{n_s} & \mathcal{A}_{I\Gamma}^{n_s}\mathcal{R}_{n_s} \\ \mathcal{R}_1^T\mathcal{A}_{\Gamma I}^{1} & \dots & \mathcal{R}_{n_s}^T\mathcal{A}_{\Gamma I}^{n_s} & \sum_{s=1}^{n_s}\mathcal{R}_s^T\mathcal{A}_{\Gamma\Gamma}^{s}\mathcal{R}_s \end{bmatrix} \left\{ \begin{array}{c} \mathcal{U}_I^1 \\ \vdots \\ \mathcal{U}_I^{n_s} \\ \mathcal{U}_\Gamma \end{array} \right\} = \left\{ \begin{array}{c} \mathcal{F}_I^1 \\ \vdots \\ \mathcal{F}_I^{n_s} \\ \sum_{s=1}^{n_s}\mathcal{R}_s^T\mathcal{F}_\Gamma^s \end{array} \right\},$$

where

$$[\mathcal{A}_{\alpha\beta}^{s}]_{jk} = \sum_{i=0}^{L}\langle\Psi_i\Psi_j\Psi_k\rangle\mathbf{A}_{\alpha\beta,i}^{s} \quad , \quad \mathcal{F}_{\alpha,k}^{s} = \langle\Psi_k\mathbf{f}_{\alpha}^{s}\rangle.$$

Sarkar, A. Benabbou, N. and Ghanem, R., IJNME, 2009.

Block Sparsity Structure

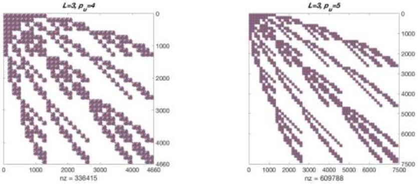

Figure : Block-sparse structures of the stochastic system matrices for a fixed mesh resolution with $L = 3$ and $p_u = 4, 5$

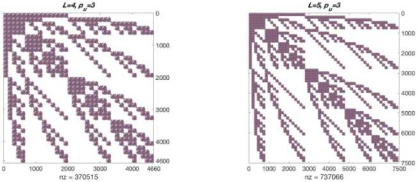

Figure : Block-sparse structures of the stochastic system matrices for a fixed mesh resolution with $p_u = 3$ and $L = 4, 5$

The Extended Interface Problem

- The Extended Schur Complement System

$$\mathcal{S}\mathcal{U}_{\Gamma} = \mathcal{G}_{\Gamma}.$$

$$\mathcal{S} = \sum_{s=1}^{n_s} \mathcal{R}_s^T [\mathcal{A}_{\Gamma\Gamma}^s - \mathcal{A}_{\Gamma I}^s (\mathcal{A}_{II}^s)^{-1} \mathcal{A}_{I\Gamma}^s] \mathcal{R}_s.$$

  - Develop parallel iterative algorithms.
  - Formulate scalable preconditioners.
  - Application to 2D and 3D Stochastic PDEs with non-Gaussian coefficients.

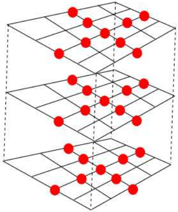

$$\mathcal{M}^{-1} = \sum_{s=1}^{n_s} {\mathcal{H}_f^s}^T [\mathcal{S}_f^s]^{-1} \mathcal{H}_f^s + \mathcal{H}_0^T [\mathcal{S}_c]^{-1} \mathcal{H}_0,$$

- Condition Number Bound of Deterministic System
    - One-level preconditioner

$$\kappa(M^{-1}S) \leq C \frac{1}{H^2} (1 + \log \frac{H}{h})^2$$

    - Two-level preconditioner

$$\kappa(M^{-1}S) \leq C (1 + \log \frac{H}{h})^2$$

Two-Level Domain Decomposition Methods for SPDEs

- Partitioning the interface nodes into remaining (■) and corner(●) nodes

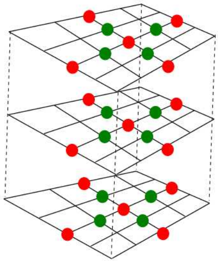

$$\mathcal{U}_\Gamma^s = \left\{ \begin{array}{c} \mathcal{U}_r^s \\ \mathcal{U}_c^s \end{array} \right\}$$

Probabilistic Balancing Domain Decomposition with Constraints

$$\begin{bmatrix} \mathcal{A}_{ii}^s & \mathcal{A}_{ir}^s & \mathcal{A}_{ic}^s \mathcal{B}_c^s \\ \mathcal{A}_{ri}^s & \mathcal{A}_{rr}^s & \mathcal{A}_{rc}^s \mathcal{B}_c^s \\ \sum_{s=1}^{n_s} \mathcal{B}_c^{s\,T} \mathcal{A}_{ci}^s & \sum_{s=1}^{n_s} \mathcal{B}_c^{s\,T} \mathcal{A}_{cr}^s & \sum_{s=1}^{n_s} \mathcal{B}_c^{s\,T} \mathcal{A}_{cc}^s \mathcal{B}_c^s \end{bmatrix} \begin{Bmatrix} \mathcal{X}^s \\ \mathcal{U}_r^s \\ \mathcal{U}_c \end{Bmatrix} = \begin{Bmatrix} \mathbf{0} \\ \mathcal{F}_r^s \\ \sum_{s=1}^{n_s} \mathcal{B}_c^{s\,T} \mathcal{F}_c^s \end{Bmatrix}$$

$$\boxed{\mathcal{M}_{NNC}^{-1} = \sum_{s=1}^{n_s} \mathcal{R}_s^T \mathcal{D}_s \mathcal{R}_s^{r\,T} [\mathcal{S}_{rr}^s]^{-1} \mathcal{R}_s^r \mathcal{D}_s \mathcal{R}_s + R_0^T [F_{cc}]^{-1} R_0,}$$

$$R_0 = \sum_{s=1}^{n_s} \mathcal{B}_c^{s\,T} (\mathcal{R}_s^c - \mathcal{S}_{cr}^s [\mathcal{S}_{rr}^s]^{-1} \mathcal{R}_s^r) \mathcal{D}_s \mathcal{R}_s.$$

$$F_{cc} = \sum_{s=1}^{n_s} \mathcal{B}_c^{s\,T} (\mathcal{S}_{cc}^s - \mathcal{S}_{cr}^s [\mathcal{S}_{rr}^s]^{-1} \mathcal{S}_{rc}^s) \mathcal{B}_c^s,$$

$$\mathcal{S}_{\alpha\beta}^s = \mathcal{A}_{\alpha\beta}^s - \mathcal{A}_{\alpha i}^s [\mathcal{A}_{ii}^s]^{-1} \mathcal{A}_{i\beta}^s, \;\; [\mathcal{A}_{\alpha\beta}^s]_{jk} = \sum_{i=0}^{L} \langle \Psi_i \Psi_j \Psi_k \rangle \mathbf{A}_{\alpha\beta,i}^s$$

Probabilistic Dual Primal Domain Decomposition

$$
\begin{bmatrix}
\mathcal{A}_{ii}^s & \mathcal{A}_{ir}^s & \mathcal{A}_{ic}^s \mathcal{B}_c^s & 0 \\
\mathcal{A}_{ri}^s & \mathcal{A}_{rr}^s & \mathcal{A}_{rc}^s \mathcal{B}_c^s & \mathcal{B}_r^{s\,T} \\
\sum_{s=1}^{n_s} \mathcal{B}_c^{s\,T} \mathcal{A}_{ci}^s & \sum_{s=1}^{n_s} \mathcal{B}_c^{s\,T} \mathcal{A}_{cr}^s & \sum_{s=1}^{n_s} \mathcal{B}_c^{s\,T} \mathcal{A}_{cc}^s \mathcal{B}_c^s & 0 \\
0 & \sum_{s=1}^{n_s} \mathcal{B}_r^s & 0 & 0
\end{bmatrix}
\begin{Bmatrix}
\mathcal{U}_i^s \\ \mathcal{U}_r^s \\ \mathcal{U}_c \\ \Lambda
\end{Bmatrix}
=
\begin{Bmatrix}
\mathcal{F}_i^s \\ \mathcal{F}_r^s \\ \sum_{s=1}^{n_s} \mathcal{B}_c^{s\,T} \mathcal{F}_c^s \\ 0
\end{Bmatrix},
$$

$$
(\bar{F}_{rr} + \bar{F}_{rc}[\bar{F}_{cc}]^{-1}\bar{F}_{cr})\Lambda = \bar{d}_r - \bar{F}_{rc}[\bar{F}_{cc}]^{-1}\bar{d}_c,
$$

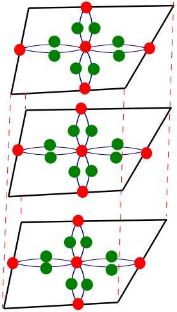

$$\mathcal{M}^{-1} = \sum_{s=1}^{n_s} \mathcal{H}_f^{s\,T} [\mathcal{S}_f^s]^{-1} \mathcal{H}_f^s + \mathcal{H}_0^T [\mathcal{S}_c]^{-1} \mathcal{H}_0,$$

	$\mathcal{H}_f^s$	$[\mathcal{S}_f^s]^{-1}$	$\mathcal{H}_0$	$[\mathcal{S}_c]^{-1}$
a	$\mathcal{R}_s^r \mathcal{D}_s \mathcal{R}_s$	$[\mathcal{S}_{rr}^s]^{-1}$	$\sum_{s=1}^{n_s} \mathcal{B}_c^{s\,T} (\mathcal{R}_s^c - \mathcal{S}_{cr}^s [\mathcal{S}_{rr}^s]^{-1} \mathcal{R}_s^r) \mathcal{D}_s \mathcal{R}_s$	$\sum_{s=1}^{n_s} \mathcal{B}_c^{s\,T} (\mathcal{S}_{cc}^s - \mathcal{S}_{cr}^s [\mathcal{S}_{rr}^s]^{-1} \mathcal{S}_{rc}^s) \mathcal{B}_c^s$
b	$\mathcal{D}_r^s \mathcal{B}_r^s$	$[\mathcal{S}_{rr}^s]^{-1}$	$\sum_{s=1}^{n_s} \mathcal{B}_c^{s\,T} \mathcal{S}_{cr} [\mathcal{S}_{rr}^s]^{-1} \mathcal{D}_r^s \mathcal{B}_r^s$	$\sum_{s=1}^{n_s} \mathcal{B}_c^{s\,T} (\mathcal{S}_{cc}^s - \mathcal{S}_{cr}^s [\mathcal{S}_{rr}^s]^{-1} \mathcal{S}_{rc}^s) \mathcal{B}_c^s$
c	$\mathcal{B}_r^{s\,T}$	$[\mathcal{S}_{rr}^s]^{-1}$	$\sum_{s=1}^{n_s} \mathcal{B}_c^{s\,T} \mathcal{S}_{cr}^s [\mathcal{S}_{rr}^s]^{-1} \mathcal{B}_r^{s\,T}$	$\sum_{s=1}^{n_s} \mathcal{B}_c^{s\,T} (\mathcal{S}_{cc}^s - \mathcal{S}_{cr}^s [\mathcal{S}_{rr}^s]^{-1} \mathcal{S}_{rc}^s) \mathcal{B}_c^s$

a) Neumann-Neumann with Coarse grid, b) Primal-Primal,c) Dual-Primal Operator.

Investigated numerical and parallel scalabilities:

Subber, W. and Sarkar, A., JCP, 2014

Subber, W. and Sarkar, A., CMAME, 2013

- Model Problem:

$$\begin{aligned} -\nabla \cdot \left(\, c_d(\mathbf{x},\theta) \;\; \nabla u(\mathbf{x},\theta) \, \right) &= F(\mathbf{x}), && \Omega \times \mathcal{W}, \\ u(\mathbf{x},\theta) &= 0, && \delta\Omega \times \mathcal{W}, \end{aligned}$$

- Diffusion coefficient c_d modelled as a lognormal process with the underlying a Gaussian process having mean μ, variance σ^2 and exponential covariance function C (on a 2D domain).

$$C(x_1, y_1; x_2, y_2) = \sigma^2 \; e^{-|x_2 - x_1|/b_1 - |y_2 - y_1|/b_2},$$

Intrusive SSFEM System Matrix: Block-Sparsity Structures

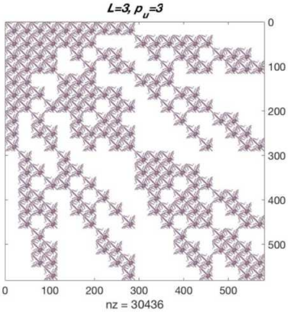

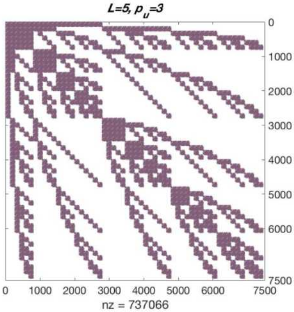

Intrusive system matrices for fixed mesh resolution $N \approx 150$, fixed order of expansion $P_u = 3$ with $L = 4$ and $L = 5$.

Errors Analysis of PCE Coefficients of Solution Process: Intrusive Vs Non-Intrusive

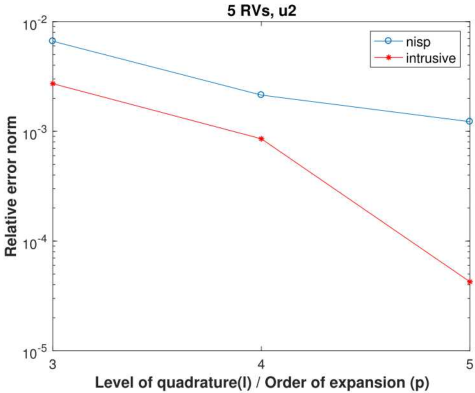

Relative error norm $= \frac{\|u_{iH} - u_{ih}\|}{\|u_{iH}\|}$, 5 random variables, error in $(\hat{\mathbf{u}}_2)$, coarse mesh ($N \approx 150$)

Scalability with Number of Stochastic Dimensions: Intrusive Vs Non-Intrusive (Sparse Grid)

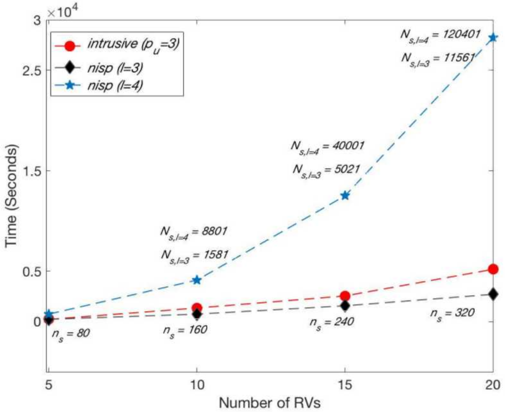

Fixed mesh resolution (52704 nodes and 105410 elements) and third order PCE for intrusive. Smolyak sparse grid with $l = 3$ and $l = 4$ for non-intrusive.

Scalability With Respect to Number of Random Variables: NNC/BDDC

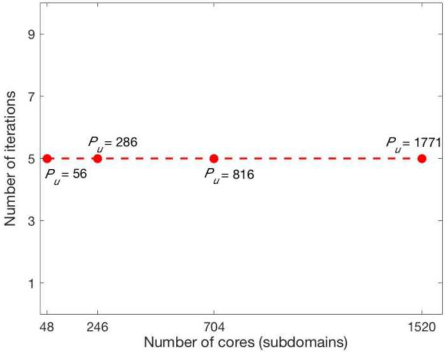

Fixed mesh resolution (52704 nodes and 105410 elements), fixed problem size per subdomain ($\approx$ 60,000) and third order PCE (linear system of order max. $\approx$ 93 million)

Scalability With Respect To Number of Random Variables: NNC/BDDC

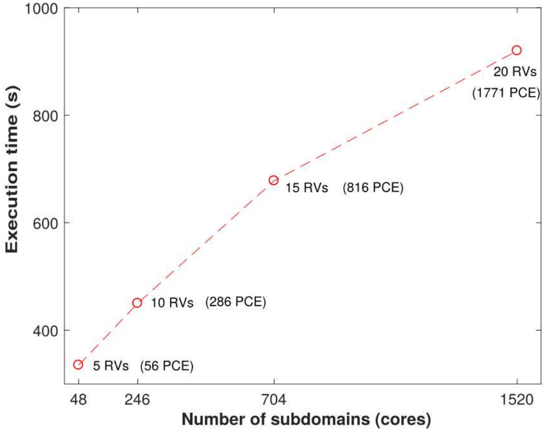

Fixed mesh (52704 nodes and 105410 elements), fixed problem size per subdomain ($\approx$ 60,000) and third order PCE

Parallel Scalability (Strong): NNC/BDDC

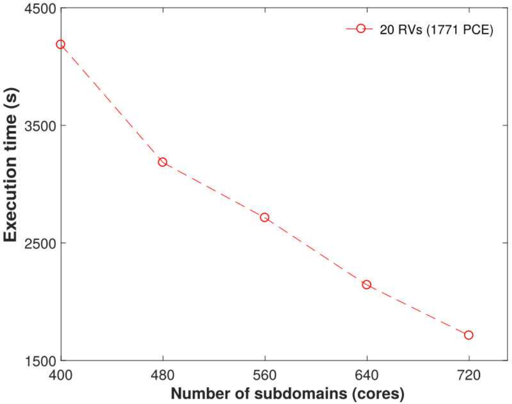

Fixed global problem, mesh with (52704 nodes and 105410 elements) and number of PCE terms $P_u = 1771$.

Scalability using Large-Scale HPC Cluster

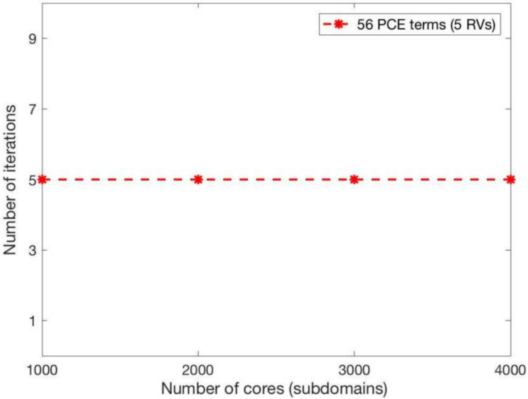

For the fixed mesh resolution (0.332 million nodes and 0.664 million elements.) and fixed number of PCE terms ($P_u = 56$).

Scalability using Large-Scale HPC Cluster

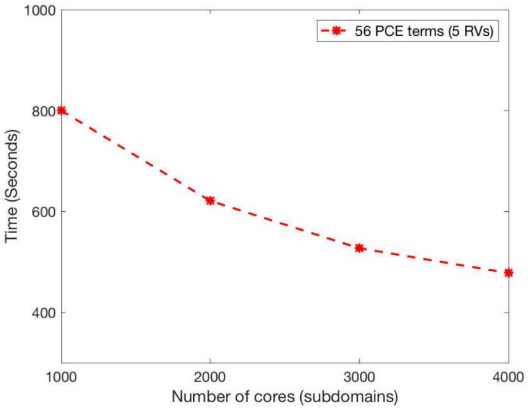

For the fixed mesh resolution (0.332 million nodes and 0.664 million elements.) and fixed number of PCE terms ($P_u = 56$).

Probabilistic Coarse Grid in Three Dimensions:

Extended Wirebasket Grid

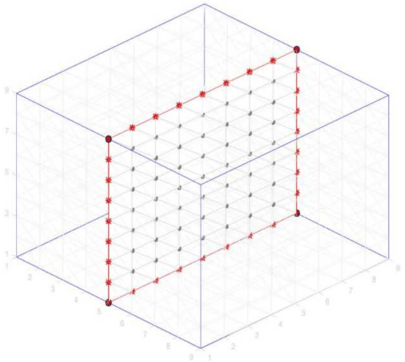

Schematic representation of a simple wirebasket coarse grid for a cube partitioned into two subdomains. (-) for the global interface edge, (•) for vertices ($\star$) for interface-edges and (•) for interface-faces.

Probabilistic Coarse Grid in Three Dimensions:

Extended Wirebasket Grid

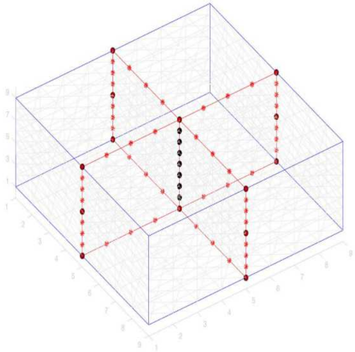

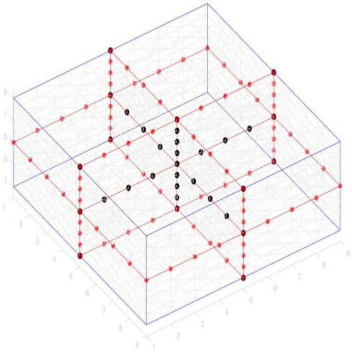

Schematic representation of the wirebasket coarse grid (consist of • and $\star$) for a cube partitioned into four and eight subdomains (exclude interface-edges $\star$ to get vertex-grid).

Deterministic Setting: Condition Number Bound

Vertex vs Wirebasket-based Methods

For the vertex-based method in two dimensions

$$\kappa \leq C(1 + \log(H/h))^2,$$

For the vertex-based method in three dimensions

$$\kappa \leq C(H/h)(1 + \log(H/h)).$$

For the wirebasket-based methods in three dimensions

$$\kappa \leq C(1 + \log(H/h))^2.$$

$$\mathcal{F}_{WW}\,\mathcal{U}_W = d_W,$$

$$\mathcal{F}_{WW} = \sum_{s=1}^{n_s} {\mathcal{B}_W^s}^{\mathrm{T}} \Big(\mathcal{S}_{WW}^s - \mathcal{S}_{WF}^s [\mathcal{S}_{FF}^s]^{-1} \mathcal{S}_{FW}^s \Big) \mathcal{B}_W^s,$$

$$d_W = \sum_{s=1}^{n_s} {\mathcal{B}_W^s}^{\mathrm{T}} \Big(f_W^s - \mathcal{S}_{WF}^s [\mathcal{S}_{FF}^s]^{-1} f_F^s \Big).$$

BDDC/NNC Preconditioner using Extended Wirebasket:

$$\mathcal{M}_{NNW}^{-1} = \sum_{s=1}^{n_s} \mathcal{R}_s^{\mathrm{T}} \mathcal{D}_s ({\mathcal{R}_s^F}^{\mathrm{T}} [\mathcal{S}_{FF}^s]^{-1} \mathcal{R}_s^F) \mathcal{D}_s \mathcal{R}_s + \mathcal{R}_0^{\mathrm{T}} [\mathcal{F}_{WW}]^{-1} \mathcal{R}_0.$$

$$\mathcal{R}_0 = \sum_{s=1}^{n_s} {\mathcal{B}_W^s}^{\mathrm{T}} (\mathcal{R}_s^W - \mathcal{S}_{WF}^s [\mathcal{S}_{FF}^s]^{-1} \mathcal{R}_s^F) \mathcal{D}_s \mathcal{R}_s,$$

Numerical Experiments: Wirebasket based BDDC/NNC solver

- Model Problem: Diffusion equation in three dimensions

$$
\begin{aligned}
-\nabla \cdot \left(\; c_d(\mathbf{x},\theta) \;\; \nabla u(\mathbf{x},\theta) \; \right) \;&=\; F(\mathbf{x}), \qquad \Omega \times \mathcal{W}, \\
u(\mathbf{x},\theta) \;&=\; 0, \qquad\qquad \delta\Omega \times \mathcal{W},
\end{aligned}
$$

- Diffusion coefficient c_d modeled as a lognormal process with the underlying a Gaussian process having mean μ, variance σ^2 and exponential covariance function C (on a 3D domain),

$$C(x_1, y_1, z_1; x_2, y_2, z_2) = \sigma^2 e^{-|x_2 - x_1|/b_x - |y_2 - y_1|/b_y - |z_2 - z_1|/b_z}.$$

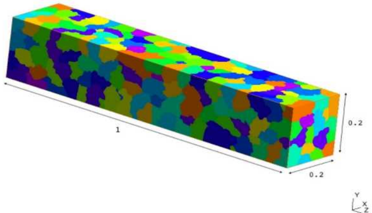

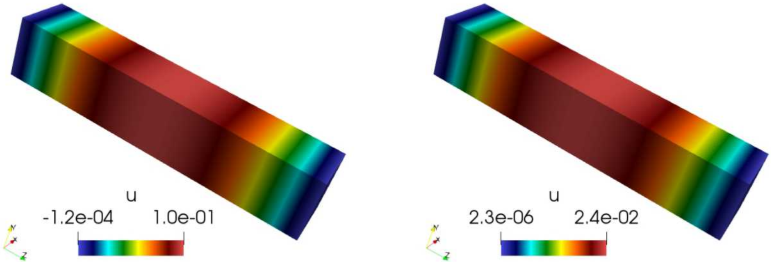

Figure : Mean and standard deviation of the solution process.

Characteristics of the Solution Process: Diffusion Equation in Three Dimensions

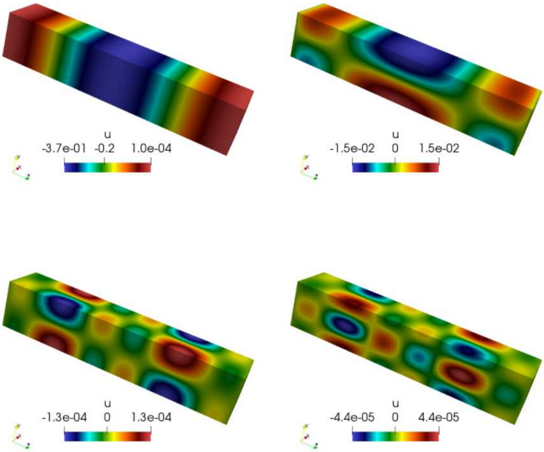

Selected PCE coefficients of the solution process.

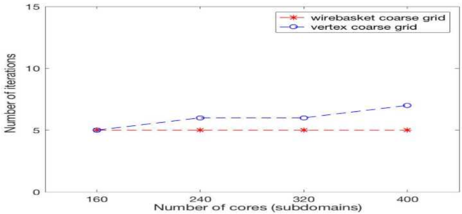

Figure : Iteration count versus number of subdomains for the fixed mesh resolution with fixed number of PCE terms.

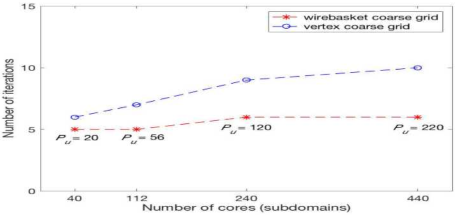

Figure : Iteration count versus number of subdomains for fixed problem size per subdomain with increasing number of PCEs (fixed mesh resolution).

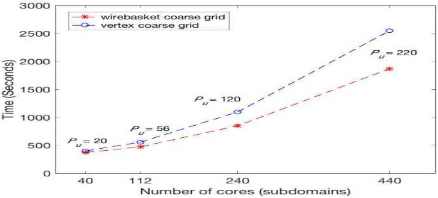

Figure : Execution time versus number of subdomains for fixed problem size per subdomain with increasing number of PCEs (fixed mesh resolution).

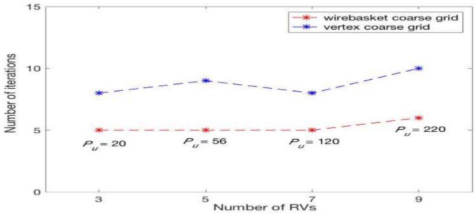

Figure : Iteration count versus number PCE terms for the fixed mesh resolution with fixed number of subdomains.

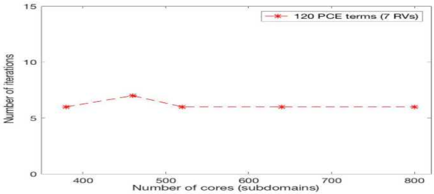

Figure : Iteration count versus number of subdomains for the fixed mesh resolution with fixed number of PCE terms.

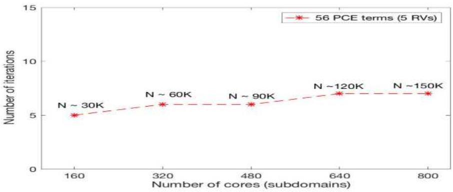

Figure : Iteration count versus number of subdomains for the fixed problem size per core with increasing mesh resolution (fixed number of PCE terms).

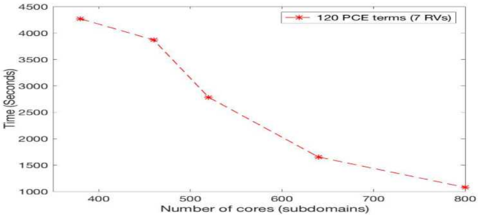

Figure : Execution time versus number of subdomains with the fixed mesh resolution and the number of PCE terms.

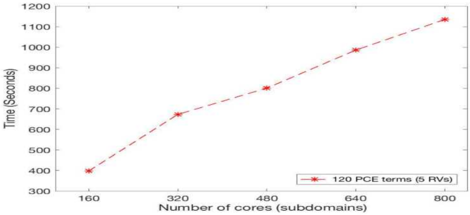

Figure : Execution time versus number of subdomains for the fixed problem size per core with increasing mesh resolution (fixed number of PCE terms).

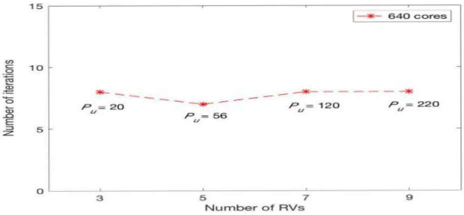

Figure : Iteration count versus number PCE terms for the fixed mesh resolution with fixed number of subdomains.

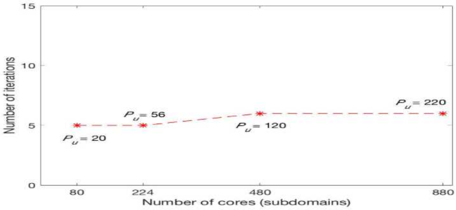

Figure : Iteration count versus number of subdomains for the fixed problem size per core with increasing number of PCE terms (fixed mesh resolution).

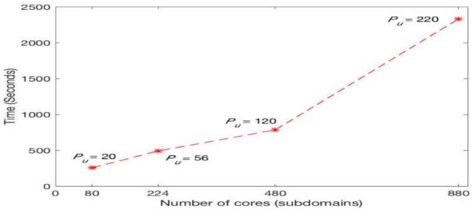

Figure : Execution time versus number of subdomains for fixed problem size per subdomain with increasing number of PCEs (fixed mesh resolution).

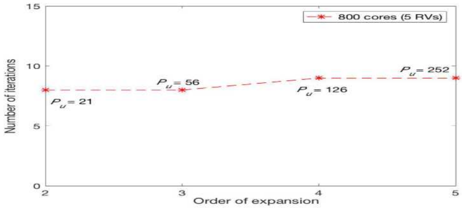

Figure : Iteration count versus order of expansion for the fixed mesh resolution with fixed number of subdomains (fixed number of RVs).

Numerical Experiments: Wirebasket based BDDC/NNC solver for Coupled PDE System

- Model Problem: Equations of Linear Elasticity in 3D,

$$-\nabla \cdot \sigma\big(\mathcal{U}(\mathbf{x},\theta)\big) = F(\mathbf{x}) \quad in \quad \mathcal{D},$$
$$\sigma\big(\mathcal{U}(\mathbf{x},\theta)\big) \cdot \hat{\mathbf{n}} = b_T \quad on \quad \Gamma_1 = \delta\mathcal{D}\backslash\Gamma_0,$$
$$\mathcal{U}(\mathbf{x},\theta) = 0 \quad on \quad \Gamma_0.$$

  Where the stress tensor, σ can be written as,

$$\sigma\big(\mathcal{U}(\mathbf{x},\theta)\big) = \lambda\big(\nabla \cdot \mathcal{U}(\mathbf{x},\theta)\big)I + 2\mu\epsilon\big(\mathcal{U}(\mathbf{x},\theta)\big),$$

  where $\lambda = \frac{E\nu}{(1+\nu)(1-2\nu)}$ and $\mu = \frac{E}{2(1+\nu)}$ are Lamé elasticity parameters.

- Young's modulus E is modeled as a lognormal stochastic process (similar to the previous case).

Characteristics of the Solution Process: Equations of Linear Elasticity in Three Dimensions

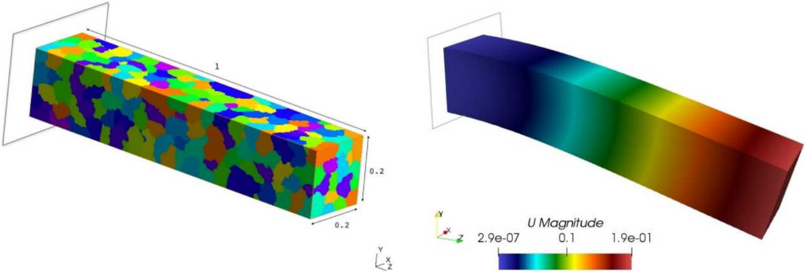

Mean magnitude of the beam deflection subjected to self-weight

Characteristics of the Solution Process:

Equations of Linear Elasticity in Three Dimensions

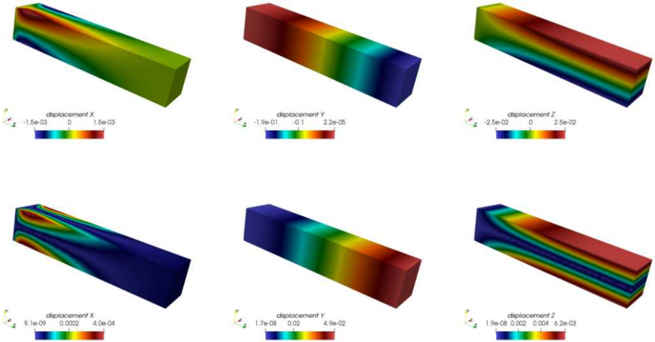

x, y and z components of the mean and standard deviation of the solution process.

Characteristics of the Solution Process:
Equations of Linear Elasticity in Three Dimensions

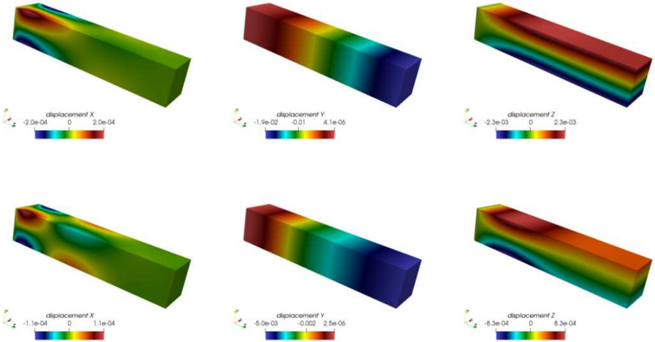

x, y and z components of the selected PCE coefficients of the solution process.

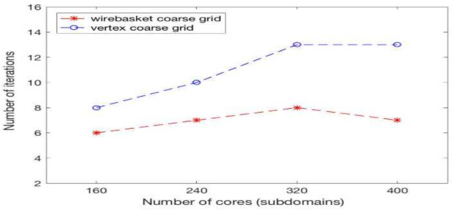

Figure : Iteration count versus number of subdomains for the fixed mesh resolution with fixed number of PCE terms.

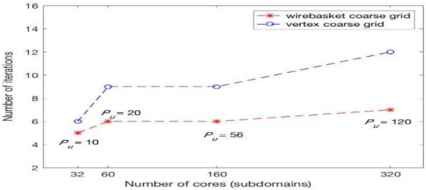

Figure : Iteration count versus number of subdomains for fixed problem size per subdomain with increasing number of PCEs (fixed mesh resolution).

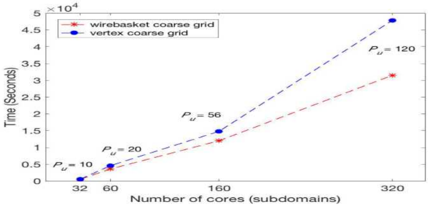

Figure : Execution time versus number of subdomains for fixed problem size per subdomain with increasing number of PCEs (fixed mesh resolution).

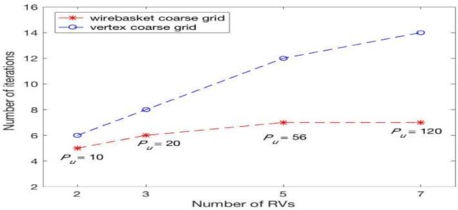

Figure : Iteration count versus number of PCE terms for the fixed mesh resolution with fixed number of subdomains.

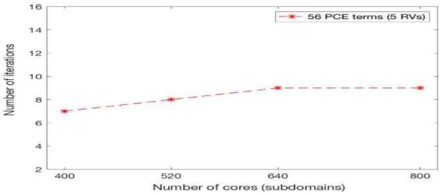

Figure : Iteration count versus number of subdomains for the fixed mesh resolution with fixed number of PCE terms.

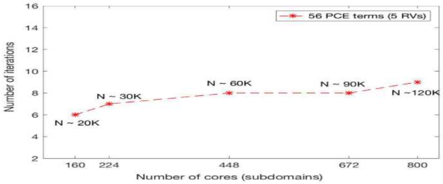

Figure : Iteration count versus number of subdomains for the fixed problem size per core with increasing mesh resolution (fixed number of PCE terms).

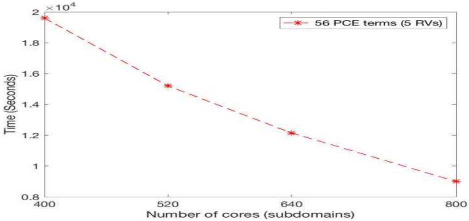

Figure : Execution time versus number of subdomains with the fixed mesh resolution and the number of PCE terms.

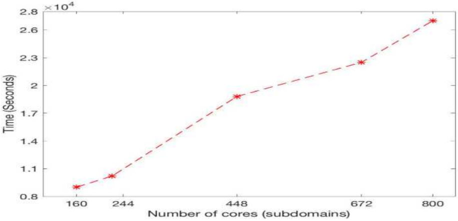

Figure : Execution time versus number of subdomains for the fixed problem size per core with increasing mesh resolution (fixed number of PCE terms).

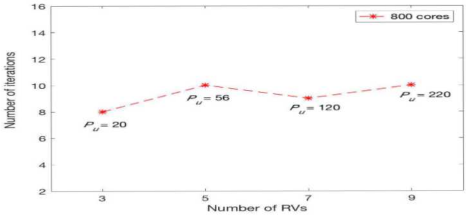

Figure : Iteration count versus number of PCE terms for the fixed mesh resolution with fixed number of subdomains.

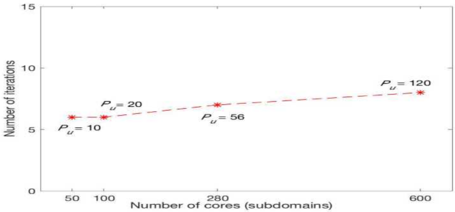

Figure : Iteration count versus number of subdomains for the fixed problem size per core with increasing number of PCE terms (fixed mesh resolution).

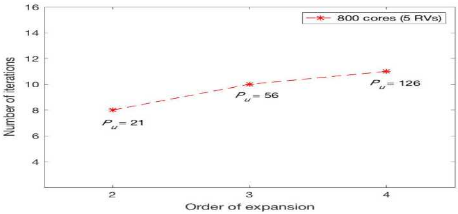

Figure : Iteration count versus order of expansion for the fixed mesh resolution with fixed number of subdomains (fixed number of RVs).

Conclusion

- Development of parallel PCKF that exploits available two-level domain decomposition algorithms for SPDEs.
- Distributed implementation and scalability studies of the parallel PCKF using a stationary stochastic diffusion problem.

Acknowledgment

- Financial contributions
  - Natural Sciences and Engineering Research Council of Canada
  - Canada Research Chair Program
  - Canada Foundation of Innovation
  - Ontario Innovation Trust